JOURNAL OF VIROLOGY, July 1991, p. 3538–3546
0022-538X/91/073538-09$02.00/0

Vol. 65, No. 7

Simian Immunodeficiency Virus Negative Factor Suppresses the Level of Viral mRNA in COS Cells

THOMAS M. J. NIEDERMAN, WEN HU, AND LEE RATNER*

Departments of Medicine and Molecular Microbiology, Washington University School of Medicine, Box 8125, 660 South Euclid, St. Louis, Missouri 63110

Received 20 August 1990/Accepted 29 March 1991

The *nef* gene is conserved among all human and simian lentiviruses. However, the amino acid similarity between simian immunodeficiency virus (SIV) and human immunodeficiency virus type 1 NEF is only 38%. To assess the role of SIV NEF on virus replication and compare its activity with that of its human immunodeficiency virus type 1 counterpart, we examined the activity of an intact *nef* gene from proviral clone pSIV 102, an isolate from SIV-MAC-251-infected cells. Proviral clone pSIV BA was constructed by introducing a premature termination codon at codon 40 of the *nef* gene without altering the predicted amino acid sequence of the overlapping *env* gene. These two clones were transfected into CD4$^-$ COS cells, and virus replication was monitored by p27 enzyme-linked immunosorbent assay kits. In seven independent experiments, clone pSIV BA afforded two- to sixfold greater levels of viral antigen compared with those in clone pSIV 102 and two- to sixfold-increased levels of viral mRNAs as indicated with Northern (RNA) blot and S1 nuclease protection analyses. Nuclear run-on assays demonstrated a two- to threefold increased rate of RNA synthesis with nuclei isolated from cells transfected with pSIV BA compared with that from cells transfected with pSIV 102. In contrast, there was no apparent destabilization of SIV mRNAs by NEF, as measured in dactinomycin-treated cells. This study demonstrates that SIV NEF is a negative regulator of virus replication and acts by suppressing the level of mRNA synthesis and accumulation in COS cells.

Simian immunodeficiency virus (SIV) is closely related to human immunodeficiency virus types 1 (HIV-1) and 2 (HIV-2) (5, 25). Both SIV and HIV include an open reading frame at the 3′ end of their genomes, the protein product of which has been named negative factor (NEF) (8). There is considerable amino acid sequence polymorphism, up to 17%, among the *nef* gene products of different HIV-1 strains (22, 26). However, there is a 62% amino acid sequence difference between the NEF proteins of SIV and those of HIV-1 (Fig. 1). Moreover, SIV NEF contains 250 amino acids, whereas HIV-1 NEF contains only 206 amino acids. Although *nef* is not required for virus replication or cytopathic effects in cultured cells (6), the gene has been conserved within all HIV and SIV genomes, which suggests that NEF serves an important function.

We and others have found that HIV-1 NEF suppresses virus replication (1, 2, 9, 16, 20, 24, 28). NEF mediates this suppression at the level of viral transcription (1, 24). However, others have been unable to demonstrate this negative effect (15, 19), indicating that NEF effects may be extremely sensitive to experimental conditions.

In this study, the role of SIV NEF on the replication of SIV-MAC was examined in the CD4$^-$ COS cell line. Although SIV and HIV-1 NEF proteins have only 38% sequence similarity, the two proteins mediate downregulation of virus production by suppressing the rate of viral transcription and mRNA accumulation. SIV *nef*-positive and -negative proviral clones will be useful in assessing the physiologic role of NEF in macaques infected with virus derived from these clones. This animal model may then contribute to our understanding of viral latency in vivo.

* Corresponding author.

MATERIALS AND METHODS

DNA clones. Clone PK102 (kindly provided by B. Hahn, University of Alabama at Birmingham School of Medicine) contains a full-length SIV genome cloned into bacteriophage lambda gt wes (14). Lambda PK102 DNA was digested with *Eco*RI and cloned into the *Eco*RI site of the plasmid expression vector pSV2gpt (21) to produce clone pSIV 102 ERL. This clone has four *Sac*I sites, two in the SIV genome (nucleotides [nt] 5731 and 9208) and two in the cellular flanking sequences. Clone pSIV 102 SDS was obtained from pSIV 102 ERL by removing the 3.5-kb *Sac*I fragment and destroying the two *Sac*I sites in the flanking sequence by excising the 0.3-kb sequence between the two sites and annealing a *Sal*I-*Sac*I adapter that destroys the *Sac*I site. A full-length, proviral clone with an intact *nef* gene, pSIV 102, was constructed by returning the 3.5-kb *Sac*I fragment to clone pSIV 102 SDS.

To generate a *nef* mutant proviral clone that is otherwise isogenic, the 3.5-kb *Sac*I fragment was subcloned into the plasmid vector pUC19 (Pharmacia) to form pUC19-SIV 3.5. Polymerase chain reaction mutagenesis was performed with a primer overlapping the *Bgl*II site (nt 9100) and a mutant primer overlapping the *Avr*II site (nt 9184), GGTGGAAGAT GGATCTTAGCAATCCCTAGGAGG, which contains a C-to-T transition and a C-to-A transversion, which introduce a termination codon at *nef* amino acid position 40 without altering the amino acid sequence of the overlapping *env* gene (Fig. 2). The nucleotide changes also eliminated the *Bam*HI site at nt 9170 by converting the sequence GGATCC to GGATCT. The mutation was confirmed by restriction enzyme digestion and sequence analysis. In addition, sequence analysis of the entire *nef* gene of clones pSIV 102 and pSIV BA confirmed that no additional cloning artifacts had occurred. The mutant *Bgl*II-*Avr*II fragment was substituted into the corresponding sites in pUC SIV 3.5. The mutant 3.5-kb *Sac*I fragment from pUC SIV 3.5 was inserted into

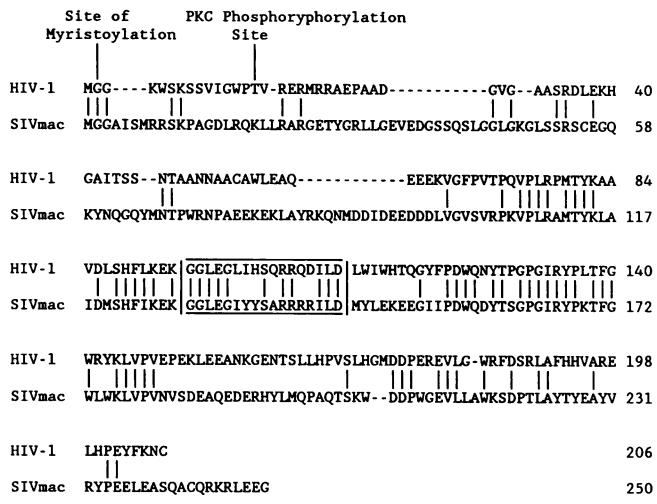

FIG. 1. Amino acid alignment of the NEF proteins derived from HIV-1 (HXB2/3gpt [24, 26]) and SIV isolate 102 (derived from SIV MAC-251 [22]). Based on this alignment, there is a 38% sequence similarity between HIV-1 NEF and SIV NEF. Both forms of NEF may be myristoylated and share sequence similarity to the nucleotide binding domain of G proteins (boxed sequences).

clone pSIV 102 SDS to generate the *nef*-negative clone pSIV BA.

The chloramphenicol acetyltransferase (CAT) expression plasmid pSV2CAT was described previously (10). The actin cDNA clone was kindly provided by J. Milbrandt (4). The *Alu*I probe was derived from a c-*sis* genomic clone, pL33M (17). The neomycin resistance gene (*neo*) expression clone pCB6 utilizes the simian virus 40 early promoter to express *neo* mRNA and was kindly provided by Evan Sadler, Howard Hughes Medical Institute.

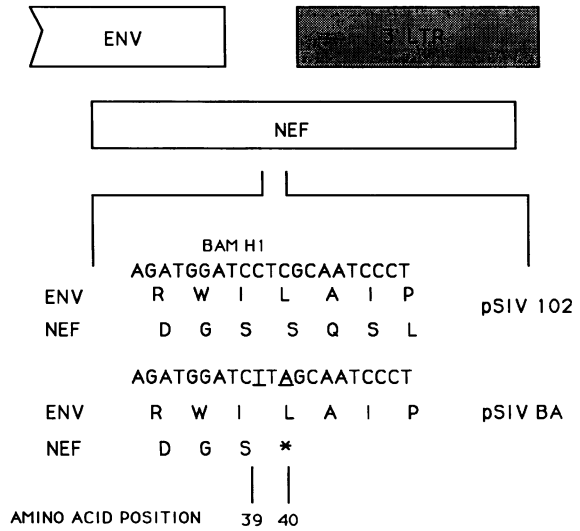

FIG. 2. Construction of *nef* mutant clone pSIV BA from wild-type clone pSIV 102. A premature termination codon was engineered at codon 40 of the *nef* gene by using polymerase chain reaction site-directed mutagenesis with a synthetic oligonucleotide spanning the mutated region. The truncated NEF protein contains only the first 39 amino acids, but the ENV protein is unaffected by the mutation since *env* and *nef* lie in different reading frames.

DNA transfection and cells. COS-7 cells are derived from African green monkey kidney cells, which do not express CD4 molecules at the cell surface and therefore cannot be infected by SIV. These cells were used because they are easily transfected and provide a system for examining the role of *nef* in a system not complicated by the possibility of multiple rounds of reinfection by viruses generated during transfection.

Proviral DNAs for transfections were purified twice by cesium chloride density centrifugation. DNA concentration was determined by optical absorption measurements and confirmed by using agarose gel electrophoresis with ethidium bromide staining. DNA clones were transfected by diluting the DNA in 4.5 ml of Dulbecco modified Eagle medium (DME) and adding 0.5 ml of a DEAE-dextran solution containing 70 ml of DME, 25 ml of 1 M Tris (pH 7.3), and 5 ml of 25-mg/ml DEAE-dextran (Sigma Chemical Co.). After the DNA solution was mixed, it was added to 60 to 80% confluent COS-7 cells on 100-mm tissue culture plates. After 4 h, the DNA solution was replaced by 5 ml of 100 μM chloroquine (Sigma) in DME supplemented with 10% fetal calf serum, 50 U of penicillin per ml, 50 μg of streptomycin per ml, and 1 mM pyruvate (DME-S). After 2 h, the cells were shocked for 2.5 min at room temperature with 2 ml of 10% dimethyl sulfoxide in DME-S, washed with phosphate-buffered saline (PBS), and cultured with DME-S at 37°C in a 5% CO_2 atmosphere.

Detection of p27^{gag}core protein. Cell-free supernatants of transfected COS cells were analyzed according to the protocols of the manufacturers with a SIV p27 enzyme-linked immunosorbent assay (ELISA) kit (Coulter) or an HIV-1 p24 kit (Abbott) with significant immunological cross-reactivity for SIV-MAC p27^{gag} antigen.

Detection of SIV proteins. At 60 h posttransfection, COS cells were metabolically labeled for 6 h with 500 μCi of [^{35}S]methionine and [^{35}S]cysteine (ICN; specific activity, >1,000 Ci/mmol) in 3 ml of methionine- and cysteine-free DME supplemented with 5% dialyzed fetal calf serum. Cells were washed and harvested by scraping in PBS, and the cell pellet was solubilized in 750 μl of protein-solubilizing buffer (0.1% SDS, 0.5% deoxycholate, 1.0% Triton X-100 [Sigma] in PBS). A 200-μl aliquot of solubilized cells was precleared with uninfected macaque serum and then immunoprecipitated with 2 μl of serum from an SIV-infected macaque (kindly provided by R. Desrosiers, New England Primate Research Center). Immunoprecipitates were washed and subjected to 7.5 to 20% gradient sodium dodecyl sulfate (SDS)–polyacrylamide gel electrophoresis (PAGE). The gels were fixed, enhanced with Amplify (Amersham), dried, and exposed to Kodak XAR-5 film at −90°C.

RNA analyses. (i) Northern blot analysis. COS cells were washed with PBS and harvested by scraping, and RNA was isolated as described previously (3). RNA was denatured at 65°C for 10 min, electrophoresed on a 1.3% agarose–formaldehyde gel, and transferred to a Nitroplus 2000 hybridization membrane (Micron Separations Inc.). Filters were baked in vacuo at 80°C for 90 min and prehybridized for 2 h in 50% formamide–5× SSC (1× SSC is 0.15 M NaCl plus 0.015 M sodium citrate)–1% SDS–50 mM $NaPO_4$ (pH 7.5)–5× Denhardt medium–200 μg of yeast tRNA per ml–50 μg of sheared salmon sperm DNA per ml. Filters were probed for 18 h at 37°C with random hexamer primer-labeled fragments generated from the internal 3.5-kb *Sac*I fragment from clone pSIV 102 or from the 2.0-kb *Hin*dIII fragment of the actin cDNA clone. Filters were washed three times at 65°C in 0.5× SSC–0.1% SDS and exposed to Kodak XAR-5

film at −90°C. Ten percent of the cells were saved for CAT activity analysis.

(ii) S1 nuclease protection assay. DNA probes were constructed by digesting clone pSIV 102 with *Stu*I, isolating the 590-bp fragment extending from nt 369 to 959, and end labeling with [γ-^{32}P]ATP (ICN; specific activity, 3,000 Ci/mmol [1 mCi = 37 mBq]) or by digesting clone pSIV 102 with *Ava*I (nt 1494), end labeling, digesting with *Bsu*36I, and isolating the 1.4-kb *Bsu*36I-to-*Ava*I fragment extending from nt 95 to 1494. A probe for *neo*-specific mRNA was generated by end labeling the 0.65-kb *Ava*II-to-*Pvu*II fragment, which is contained exclusively in the *neo* gene, from the *neo* expression clone. Total cellular RNA (12 or 18 μg) from transfected COS cells was hybridized to either probe at 56°C for 90 min and then at 53°C for 90 min in 80% formamide–40 mM PIPES [piperazine-*N*,*N*′-bis(2-ethanesulfonic acid)] (pH 6.4)–1 mM EDTA–0.4 M NaCl. Samples were cooled to 16°C and digested for 30 min by adding 0.3 ml of ice-cold S1 buffer (0.28 M NaCl, 0.05 M sodium acetate [pH 4.6], 4.5 mM $ZnSO_4$, 20 μg of sheared salmon sperm DNA per ml) containing 1,000 U of S1 nuclease (Pharmacia) per ml. Reactions were stopped by adding 50 μl of 4.0 M ammonium acetate–0.1 M EDTA. Then 10 μg of yeast tRNA was added, and the nucleic acids were precipitated with ethanol. Precipitates were dried, suspended in 20 μl of loading buffer (38% formamide, 8 mM EDTA, 0.002% bromophenol blue, 0.002% xylene cyanol FF), and subjected to denaturing PAGE (5% polyacrylamide) with 50% urea. Gels were dried and exposed to Kodak XAR-5 film for 3 days at −90°C. Ten percent of the cells were saved for CAT activity analysis.

Nuclear run-on assays. Nuclear run-on assays were performed as described (24) with the exception that 1.0-μg samples of plasmids pL33M, pSV2gpt, and pSIV 102 were used as the cold DNA targets immobilized on the nitrocellulose filters.

Dactinomycin analysis. COS cells (70% confluent) in 75-cm flasks were transfected with 12 μg of either pSIV 102 or pSIV BA. At 24 h posttransfection, cells were trypsinized and the pSIV 102 and pSIV BA flasks were separately pooled and seeded onto 150-mm plates. At 24 h after reseeding, media was replaced with DME-S containing 5 μg of dactinomycin (Sigma) per ml, and cells were harvested for RNA at 0, 12, 24, 36, and 48 h posttransfection. Isolated RNA was subjected to Northern blot analysis and probed with hexamer primer-labeled fragments derived from the 3.5-kb *Sac*I fragment or to labeled actin sequences.

CAT assays. The pSV2CAT expression vector and the assay protocol were described previously (10).

RESULTS

pSIV 102 and pSIV BA direct the synthesis of SIV proteins. A functional SIV proviral clone with an intact *nef* gene, pSIV 102, was used to generate an otherwise isogenic *nef* mutant, pSIV BA, by polymerase chain reaction site-directed mutagenesis (Fig. 2). The predicted length of the mutant NEF protein is truncated from 250 to 39 amino acids. Proviral clones pSIV 102 and pSIV BA and negative control plasmid pSV2gpt were transfected into COS cells, which were then metabolically labeled with [^{35}S]methionine and [^{35}S]cysteine and immunoprecipitated with antiserum from an infected macaque. The cells transfected with the proviral clones demonstrate the presence of precursor and processed *gag* proteins, whereas the cells transfected with the negative control do not (Fig. 3). Equal volumes of cell lysate were applied to the gel; however, Bradford protein analysis and densitometric scanning of background bands indicate that protein concentration was 3.5-fold greater in the pSIV 102 sample than in the pSIV BA sample. Additionally, densitometric analysis indicates that the intensity of the p27 *gag* band was 1.5-fold greater in the pSIV 102 lane than in the pSIV BA lane. Therefore, in this experiment, there was a 2.3-fold suppression of p27 with clone pSIV 102 compared with that for pSIV BA. As expected, NEF protein was identified only in cells transfected with clone pSIV 102 (Fig. 3, lane 2). The apparent molecular mass of NEF protein, calculated by using the size markers indicated, was 29.5 kDa, which agrees well with the predicted molecular mass of 29 kDa.

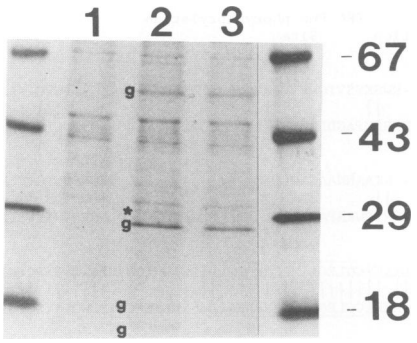

FIG. 3. Expression of SIV NEF and GAG proteins. COS cells were transfected with 10 μg of pSV2gpt (lane 1), pSIV 102 (lane 2), or pSIV BA (lane 3). At 48 h posttransfection, cells were labeled with [^{35}S]methionine and [^{35}S]cysteine and immunoprecipitated with serum from an infected macaque. Immunoprecipitated samples were then denatured and subjected to SDS–PAGE in a 7.5 to 20% gradient. *, NEF protein expressed in pSIV 102-transfected cells; g, precursor and processed *gag* proteins in pSIV 102- and pSIV BA-transfected cells.

NEF downregulates SIV replication in COS cells. To assess the role of *nef* on the replication of SIV, COS cells were transfected with proviral clones pSIV 102 and pSIV BA. Supernatants from transfected cells were solubilized and screened for viral antigens by using a p27 SIV ELISA kit (Fig. 4A) or a p24 HIV ELISA kit (Fig. 4B). In seven independent experiments with different DNA preparations and cell stocks, the clone lacking *nef* pSIV BA, consistently afforded two- to sixfold-higher levels of virus particles in the supernatant compared with those in pSIV 102. Transfection efficiency was measured by cotransfecting with pSV2CAT and measuring CAT activity in cellular protein extracts. This analysis indicated that the mean values of CAT activity were 6.1% ± 3.0%, 4.9% ± 3.0%, and 4.7% ± 1.8% for the pSV2gpt-, pSIV 102-, and pSIV BA-transfected cells, respectively. These values represent the percentage conversion to acetylated products and were in the linear range of analysis.

NEF decreases the level of SIV mRNA accumulation. To assess the step in the virus life cycle that was downregulated by NEF, Northern blot analysis was performed. COS cells were transfected with pSIV 102 or pSIV BA; at 72 h posttransfection, cells were harvested, and total cellular RNA was prepared and subjected to Northern blot analysis (Fig. 5). The level of SIV 9.0-kb mRNA was on the average 4.5-fold greater from the cells transfected with clone pSIV BA than from cells transfected with pSIV 102. Similarly, the level of the SIV 4.5-kb single-spliced *env* mRNA was threefold higher in the absence of NEF protein with pSIV BA

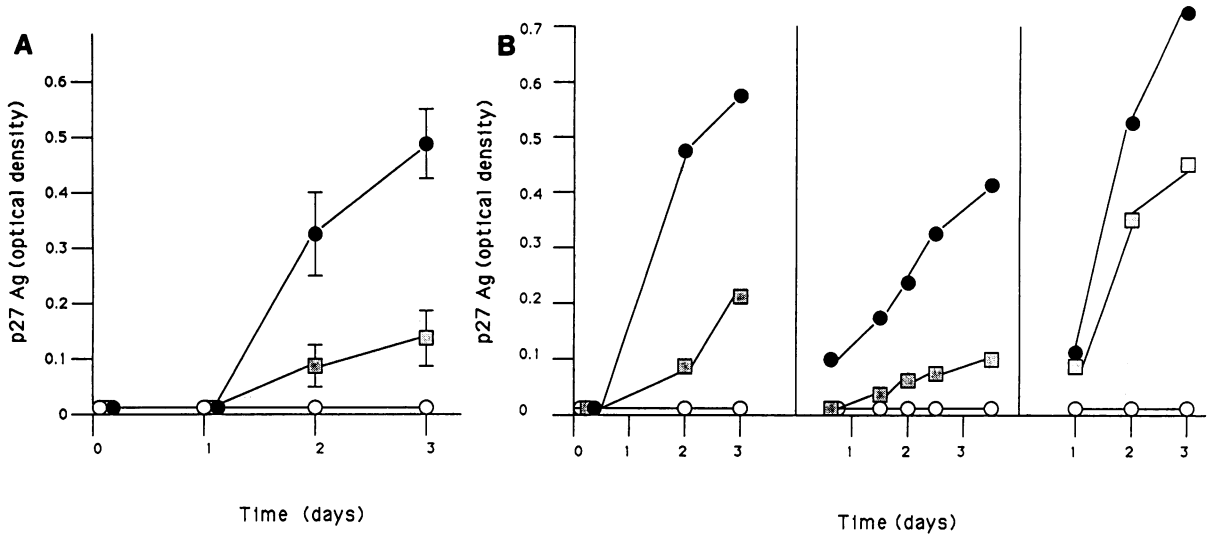

FIG. 4. NEF downregulates SIV replication in transfected COS cells. In seven independent experiments, 10 μg of either pSV2gpt, pSIV 102, or pSIV BA was transiently transfected into COS cells. An aliquot of the overlying medium was removed at the indicated times after transfection and assessed for solubilized $p27^{gag}$ core protein with (A) a Coulter SIV p27 ELISA kit or (B) an Abbott p24 HIV ELISA kit. (A) Averages of four experiments with error bars indicating 1 standard deviation from the mean. (B) Three different experiments. Transfection efficiency was monitored by cotransfecting pSV2CAT and measuring CAT activity; however, this parameter did not vary by more than 10% in any given experiment. For panel A, 1 optical density unit is approximately equal to an antigen concentration of 15 ng/ml. Symbols: ○, pSV2gpt; ▨, pSIV 102; ●, pSIV BA.

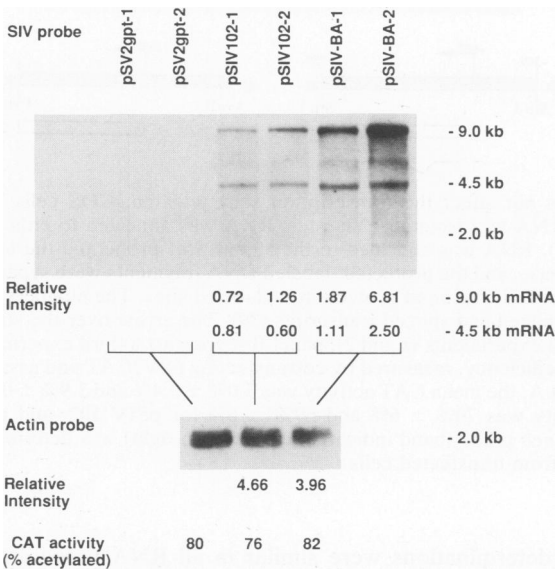

FIG. 5. SIV NEF decreases viral mRNA accumulation. COS cells were transfected with 10 μg of either pSV2gpt, pSIV 102, or pSIV BA and cotransfected with clone pSV2CAT to control for transfection efficiency. Total cellular RNA was isolated 3 days after transfection from 90% of the cells and subjected to Northern blot analysis. Protein extracts were prepared from the remaining 10% of the cells for CAT analysis. Hybridization was performed with hexamer-primed probes generated from the 3.5-kb *Sac*I fragment from clone pSIV 102. In this experiment, duplicate transfections were performed. RNAs from experiments 1 and 2 were combined equally, subjected to Northern blot analysis, and hybridized to actin sequences that demonstrated that similar amounts of RNA were applied to the gel. CAT activities were similar within the linear range of analysis.

than in the presence of NEF with pSIV 102 based on densitometry analysis of the bands. All three major viral RNA species were detected, and the presence or absence of NEF protein did not appear to alter their relative abundance. The probe used in this analysis, derived from the 3.5-kb *Sac*I fragment, hybridized weakly to the 2.0-kb double-spliced mRNAs. Hybridization of the same RNA samples to actin sequences was used to correct for differences in RNA extraction and concentration determinations. Transfection efficiency was assessed by cotransfecting the cells with pSV2CAT and was similar in all samples (Fig. 5). This analysis was repeated twice with comparable results.

S1 nuclease protection assays provided further evidence that SIV mRNA accumulation is depressed in cells transfected with the NEF-expressing proviral clone (Fig. 6). Total cellular RNA from transfected cells was hybridized with end-labeled DNA probes extending from nt 95 to 1494 (Fig. 6A) or nt 369 to 959 (Fig. 6B), where the RNA initiation (CAP) site is at nucleotide position 507. In addition to the SIV probe in Fig. 6B, an end-labeled DNA probe for *neo* mRNA was also added to the hybridization reactions (Fig. 6C). The mRNAs presented in Fig. 6C were isolated from cells cotransfected with 5 μg of the *neo* expression vector pCB6. With the longer SIV probe, in experiments 1 and 2, respectively, there were 6.6- and 4.7-fold increases in the level of the protected, correctly initiated viral RNA from cells transfected with clone pSIV BA compared with that from cells transfected with pSIV 102 (Fig. 6A). There was also a significant increase in the level of a spliced RNA species, recently described by Viglianti and coworkers (29), in cells transfected with pSIV BA compared with that in cells transfected with pSIV 102. With the shorter probe, there was a 4.4-fold increase in protected RNA of the expected size from the cells transfected with pSIV BA compared with that in cells transfected with pSIV 102 (Fig. 6B). There was also an increase in protected spliced RNA with proviral clone pSIV BA compared with that with pSIV 102. With the

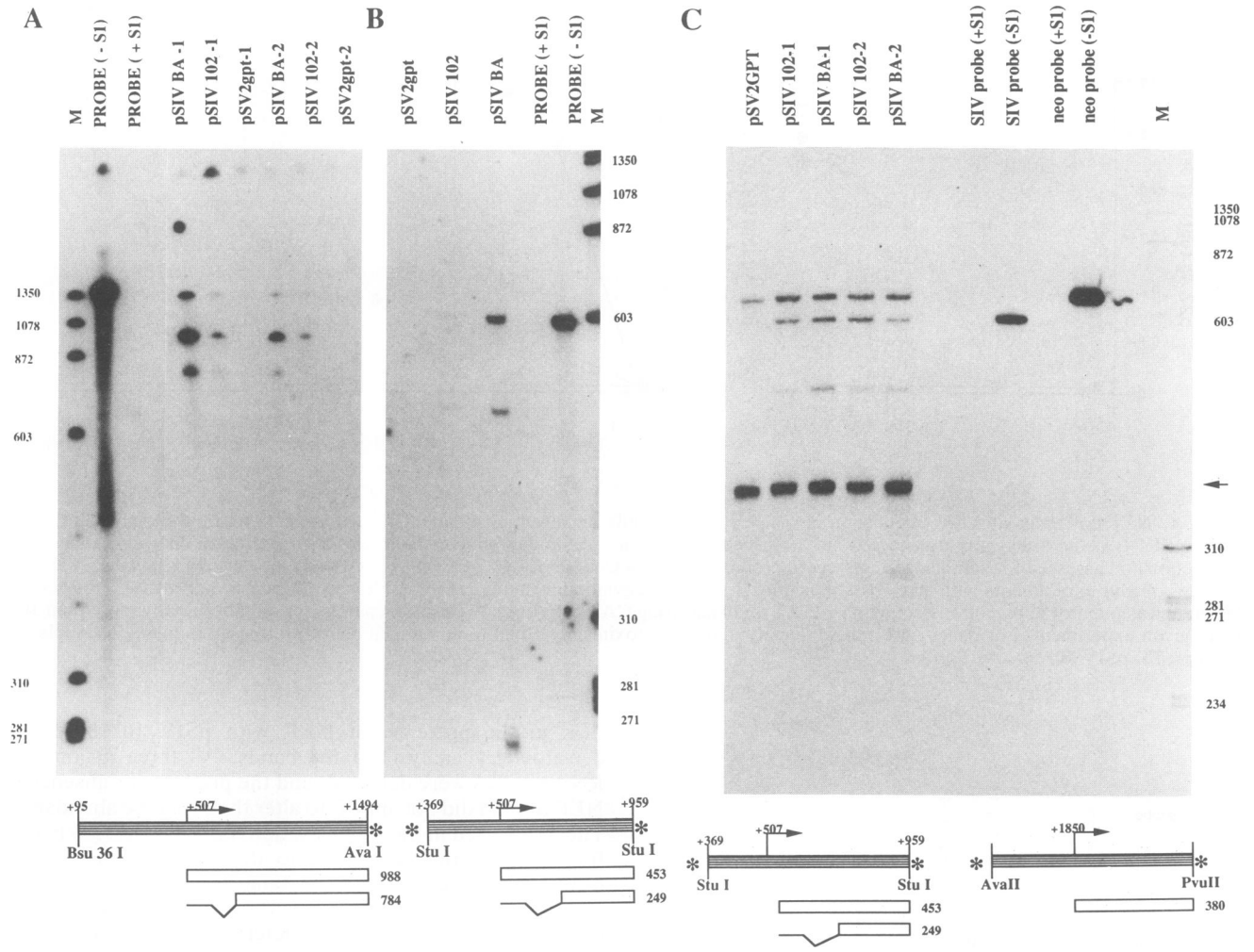

FIG. 6. SIV NEF decreases steady-state levels of SIV mRNA and does not affect the transcription start position. COS cells were transfected with proviral clones pSIV 102 and pSIV BA, and total cellular RNA was isolated 72 h later. RNA was annealed to either the *Bsu*36I (nt 94)-to-*Ava*I (nt 1494) fragment (A) or the 590-nt *Stu*I fragment (B). RNA was annealed to the 590-nt *Stu*I probe and the 655-nt *Ava*II-to-*Pvu*II *neo* probe in panel C. Samples were then digested with S1 nuclease, and the protected, labeled DNA fragments were separated on denaturing PAGE (5% polyacrylamide). Symbols: ▤, length of the probe; □, region of protection; *, labeled sites. The numbers next to the empty boxes indicate the lengths of the protected fragments of the unspliced and spliced transcripts (29). The arrow over the striped box at nt 507 indicates the RNA CAP site. Panel A represents two independent experiments (1 and 2), panel B represents a third experiment, and panel C represents two additional independent experiments. Transfection efficiency, measured by cotransfecting pSV2CAT and assaying CAT activity (percent acetylation), was determined for all transfections. In part A, the mean CAT activity was 3.0% ± 0.4% and 3.9% ± 0.7%; in part B, the activity was 3.9% and 3.4%; and in part C, the mean activity was 70% ± 6% and 69% ± 6% for pSIV 102- and pSIV BA-transfected cells, respectively. In addition, the intensity of the protected *neo* probe (band indicated by arrow on right) was determined, and the value was used to adjust the relative concentration of viral mRNAs from transfected cells.

shorter SIV probe in the experiments presented in Fig. 6C, there was a mean 2.3-fold decrease in the unspliced mRNA from pSIV 102 compared with that in mRNA from pSIV BA and a 2.1-fold decrease in the spliced mRNA species. Hybridization to the *neo* probe demonstrated similar transfection and RNA extraction efficiencies and was used to calculate the ratio of SIV to *neo* mRNAs from pSIV 102- and pSIV BA-transfected cells. Transfection efficiency, measured by cotransfection of pSV2CAT, was similar in all transfections. In the experiments shown in Fig. 6A, B, and C, the mean CAT activities were 3.0 and 3.9%, 3.9 and 3.4%, and 70 and 68% for pSIV 102 and pSIV BA, respectively. Hybridization of the RNAs to actin sequences was performed to confirm that extraction efficiency and concentration determinations were similar in all RNA preparations. The increased level of full-length protected probe in the lanes with RNA from pSIV BA-transfected cells compared with those from the pSV2gpt- or pSIV 102-transfected cells in Fig. 6 may represent effects on an aberrantly initiated transcript.

NEF suppresses the rate of SIV mRNA transcription. To determine whether the effects of NEF protein on mRNA accumulation could be accounted for at the level of RNA synthesis, nuclear run-on assays were performed. COS cells were transfected, nuclei were isolated, and preinitiated mRNA transcripts were labeled in vitro with [α-^{32}P]UTP. The ratio of hybridization of labeled RNAs to SIV sequences to that of *Alu*I sequences was twofold higher with nuclei

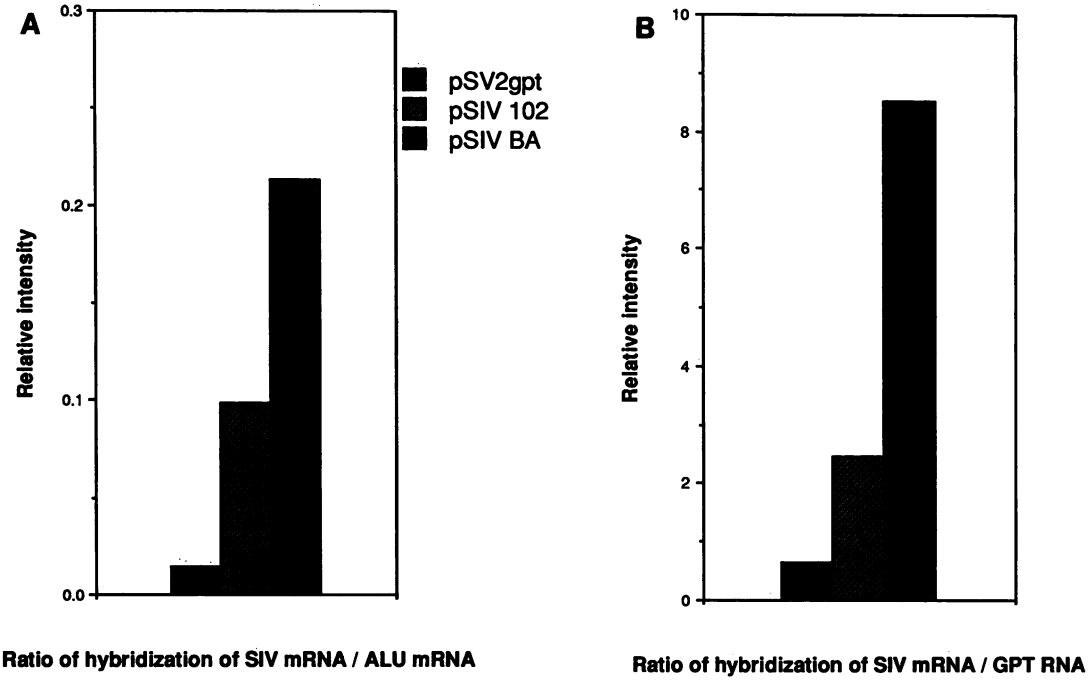

FIG. 7. SIV NEF decreases the rate of viral RNA synthesis. Nuclear run-on assays were performed with [α-^{32}P]UTP (specific activity, 3,000 Ci/mmol) to label nuclei isolated from COS cells transfected with 10 μg of pSV2gpt, pSIV 102, or pSIV BA. The nascent, labeled transcripts were hybridized to SIV sequences (pSIV 102), *Alu*I repetitive sequences (pL33M), or *gpt* sequences (pSV2gpt) to control for the efficiency of labeling, RNA yield, and transfection efficiency. Hybridization intensity was measured by densitometry and is expressed as the ratio of hybridization to SIV sequences to that to *Alu*I (A) or *gpt* (B) sequences.

isolated from pSIV BA-transfected cells than with nuclei from pSIV 102-transfected cells (Fig. 7A). The ratio of hybridization of labeled transcripts to SIV sequences to that of xanthine-guanine phosphoribosyl transferase (*gpt*) sequences was threefold greater with nuclei from pSIV BA transfected cells than with nuclei from pSIV 102-transfected cells (Fig. 7B). Hybridization to *Alu*I sequences corrects for labeling efficiency, RNA extraction, and concentration of RNA used for hybridization. Hybridization to *gpt* sequences corrects for transfection efficiency, since proviral clones pSIV 102, pSIV BA, and pSV2gpt express *gpt* mRNA at the same level. This experiment was repeated twice with similar results.

NEF does not destabilize SIV mRNA. To assess whether NEF-induced RNA degradation contributes to decreased steady-state levels of mRNAs, viral mRNA stability was measured. COS cells transfected with pSIV 102 or pSIV BA were treated with the RNA synthesis inhibitor dactinomycin and harvested 0, 12, 24, 36, and 48 h later. RNAs were subjected to Northern blot analysis, which revealed a relatively intense signal for the 4.5-kb single-spliced *env* transcript compared with that of the 9.0-kb unspliced transcript (Fig. 8); therefore, RNA measurements were performed on the *env* transcript. There was no apparent difference in the kinetics of RNA degradation in the presence (pSIV 102) or absence (pSIV BA) of an intact *nef* gene. Cells transfected with either clone displayed an RNA half-life of approximately 9 h. Hybridization of RNA to actin sequences was used to correct for RNA extraction efficiency and concentration determinations. Hybridization to c-*myc* sequences indicated that dactinomycin treatment of cells was effective in halting RNA synthesis (data not shown). The observation that the single-spliced mRNA species was more intense in this experiment than in the Northern blot in Fig. 5 may be due to the fact that these mRNAs were harvested at 48 h rather than 72 h posttransfection. Furthermore, the cells in this experiment were scraped at 24 h posttransfection and replated. It is also possible that the RNA blotting process was less efficient in this experiment than in the experiment of Fig. 5 in that the larger unspliced species failed to transfer as well. This experiment was repeated with comparable results.

DISCUSSION

Conservation of the *nef* gene in both simian and human immunosuppressive viruses suggests that the gene plays an important role in the biology of these lentiviruses. To define this role, a *nef*-positive SIV proviral clone (pSIV 102) and a *nef*-negative clone (pSIV BA) were compared. The *nef* gene product was found to suppress the rate of transcription and level of viral RNAs.

The initial comparison of the *nef*-positive and -negative proviral clones involved transfecting them into COS cells and assaying the overlying culture medium for the SIV p27 core protein. The level of p27 in the media of cells transfected with proviral clone pSIV BA was two- to sixfold higher than that of cells transfected with clone pSIV 102 (Fig. 4). This result is consistent with the role of NEF as a negative factor with respect to virus replication.

We found previously that the HIV-1 *nef* gene product did not affect the infectivity of virus particles (24). This is consistent with the data in the current study indicating that SIV NEF suppressed virus replication in cells that were unable to be infected by virus particles generated during transfections. Thus, the steps involved with the first half of the virus life cycle, i.e., virus binding, uptake, uncoating,

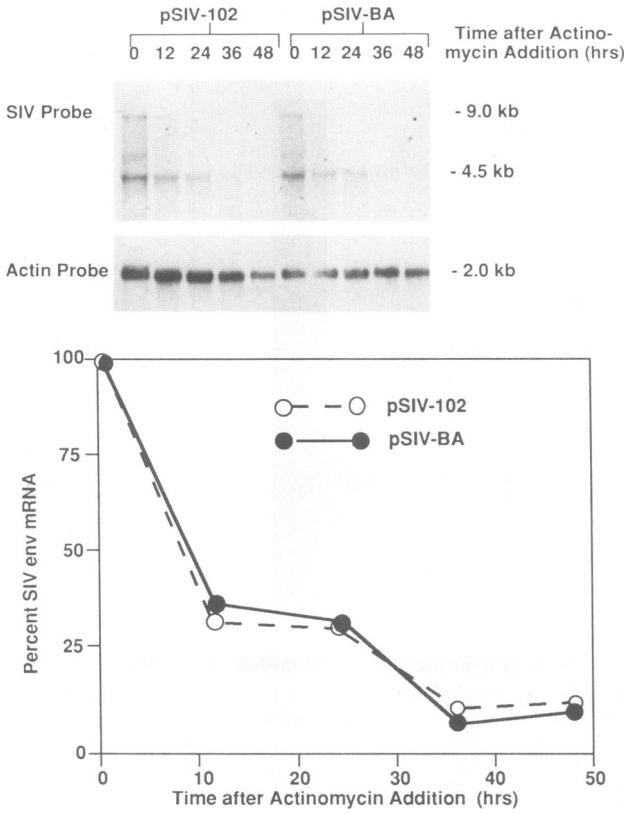

FIG. 8. SIV NEF does not destabilize SIV mRNAs. COS cells (in eight 75-mm flasks) were transfected with either clone pSIV 102 or pSIV BA. At 24 h after transfection, the COS cells were harvested and pooled with similarly transfected cells and replated onto 150-mm plates. At 24 h after replating, the cells were incubated with dactinomycin for 0 to 48 h. At the indicated times, total cellular RNA was isolated and subjected to Northern blot analysis. The blot was first hybridized with the SIV probe as in the experiment shown in Fig. 4, exposed to film, stripped of RNA, and rehybridized to an actin probe as a control for the amount of RNA loaded on the gel. In this analysis, the stability of the 4.5-kb *env* mRNA was measured because it was the predominant species. At each time point, the calculated amount of SIV mRNA was determined by densitometry and the level of *env* mRNA was adjusted to the amount of actin mRNA.

reverse transcription, and integration, are not the primary target for NEF-mediated suppression. Instead, we found that NEF was active during the second half of the virus life cycle, i.e., during transcription, RNA processing and translocation, and translation. Northern blot analysis with RNA extracted from COS cells transfected with the proviral clones showed that the steady-state levels of viral RNAs were three- to fourfold lower in the *nef*-positive clone than in the *nef*-negative clone (Fig. 5). Similar results were found with analyses of cytoplasmic or nuclear RNAs (data not shown). S1 nuclease protection analysis demonstrated a four- to sixfold suppression of correctly initiated viral mRNAs in the cells transfected with the *nef*-positive clone relative to that in the cells transfected with the *nef*-negative clone (Fig. 6).

A collection of 17 independent comparisons from 10 different experiments of viral mRNAs from pSIV 102- and pSIV BA-transfected cells is presented in Table 1. The mean suppression of viral mRNA mediated by NEF was 3.2-fold ±

TABLE 1. SIV NEF downregulates viral mRNA levels[a]

Expt	Proviral pSIV clone	Ratio[b]	mRNA suppression			CAT activity[c] (%)	Analysis
			SIV	Actin	*neo*		
1	102	2.7	0.9	1.8	8.9	64	Slot blot
	BA		2.1	1.4	6.1	74	
	102		1.3	2.3	7.2	77	
	BA		2.5	1.8	9.1	63	
2	102	1.9	2.1	1.1	7.2	44	Slot blot
	BA		2.9	1.3	9.7	50	
	102		2.4	1.5	12	49	
	BA		2.6	0.7	8.8	50	
	102		2.2	1.8	7.7	39	
	BA		1.9	0.7	7.3	50	
3	102	2.6	1.8	2.7	ND[d]	ND	Slot blot
	BA		3.6	2.8	ND	ND	
	102		3.0	1.6	ND	ND	
	BA		8.8	1.4	ND	ND	
4	102	1.7	1.4	5.3	ND	ND	Slot blot
	BA		2.3	4.8	ND	ND	
5	102	4.0	0.8	4.7	ND	76	Northern
	BA		1.5	4.0	ND	82	
	102		0.9	4.7	ND	76	
	BA		4.7	4.0	ND	82	
6	102	5.8	1.4	5.1	ND	3.4	S1 nuclease
	BA		6.2	3.9	ND	3.2	
	102		1.0	4.2	ND	2.5	
	BA		6.3	4.7	ND	4.6	
	102		0.6	5.1	ND	3.9	
	BA		3.0	3.9	ND	3.4	
7	102	3.5	3.5	5.0	ND	ND	Northern
	BA		7.1	2.9	ND	ND	
8	102	1.9	2.4	6.7	ND	ND	Northern
	BA		2.2	3.3	ND	ND	
9	102	2.7	1.0	0.9[e]	ND	ND	Run-on
	BA		2.9	1.0[e]	ND	ND	
10	102	2.6	1.5	1.4[e]	ND	ND	Run-on
	BA		2.0	0.7[e]	ND	ND	

[a] This table summarizes the data from 10 separate experiments and includes 17 different matched pairs of densitometry scans of SIV, actin, or *neo* mRNAs (expressed as relative areas under each curve) from pSIV 102- and pSIV BA-transfected COS cells. In all cases, COS cells were transfected with 10 μg of proviral DNA per 100-mm plates. These data include mRNAs that were analyzed by slot blot and Northern blot hybridization, S1 nuclease protection assays, and nuclear run-on assays. We calculated the level of viral mRNA suppression for each of the 17 matched pairs of pSIV 102 and pSIV BA values in order of the pairs from the top of the table downward. We found that the mean suppression of NEF on viral mRNA levels was 3.2-fold ± 1.6-fold, where 1.6 represents the standard deviation. In addition, the 95% confidence intervals (2.4 and 4.0) indicate that the mean of 17 random matched pairs will lie between 2.4- and 4.0-fold 95% of the time.

[b] Average ratio of the SIV densitometry values of pSIV BA divided by those of pSIV 102 multiplied by the ratio of actin densitometry values of pSIV 102 divided by those of pSIV BA-transfected cells.

[c] CAT activity (measured as percent conversion to acetylated products) of a pSV2CAT plasmid that was cotransfected with the SIV proviral clones.

[d] ND, Not done.

[e] In the nuclear run-on assays, hybridization to *Alu*I sequences served as a control for viral RNA concentration determinations instead of actin sequences.

1.6-fold, where 1.6 is the standard deviation. Ninety-five percent confidence intervals indicate that the mean suppression in any 17 matched pairs of viral mRNAs from pSIV 102- and pSIV BA-transfected cells is intermediate between 2.4- and 4.0-fold.

The observation that steady-state viral mRNA levels were decreased in the presence of *nef* suggests that *nef* either suppresses the rate of RNA synthesis or enhances the rate of RNA degradation. Therefore, nuclear run-on and dactinomycin stability studies were performed. Nuclear run-on analysis of COS cells transfected with either pSIV 102 or pSIV BA indicated that the rate of RNA synthesis was suppressed two- to threefold in the *nef*-positive clone relative to that in the *nef*-negative clone (Fig. 7). This level of transcriptional suppression could account for the differences in the steady-state level of viral mRNA in the presence or absence of NEF in that differences in the magnitude of suppression could reflect differences in experimental approaches. Analysis of viral RNA levels after dactinomycin treatment indicated that NEF did not significantly alter the rate of degradation of viral mRNA (Fig. 8).

We conclude from these experiments that SIV NEF suppresses virus replication in COS cells and that this suppression occurs at the level of viral mRNA synthesis. This study of SIV NEF parallels our previous analysis of the HIV-1 *nef* gene product (24) and the results of other investigators (1). However, others have not demonstrated a suppressive role for HIV-1 NEF on virus replication (15, 19). The discrepancy may lie in the fact that the experiments were not conducted with similar reagents in the same context. That is, Kim et al. (19) used a proviral clone that was different from that used by Ahmad and Venkatesan (1) or in our laboratory (24). Perhaps more significantly, the multiplicity of infection (MOI) varied greatly between our experiments and those of Kim et al.; we used very low MOIs whereas Kim et al. used high MOIs. It is likely that the subtle effects of NEF may be masked by the high MOI used by Kim et al. The proviral clone studied by Hammes et al. was HXB3, which contains a *nef* gene similar to the clone used in our previous experiments except that clone HXB3 contains an alanine instead of a threonine residue at amino acid position 15. Guy et al. (12) demonstrated that protein kinase C requires a threonine residue for phosphorylation at amino acid residue 15 and that this phosphorylation event may be critical for NEF activity. Currently, we are studying the role of the MOI on NEF activity with different proviral clones in an attempt to explain the discrepancies that have arisen with respect to the role of NEF on virus replication.

The precise mechanism by which NEF mediates transcriptional suppression is not known. HIV-1 NEF has not yet been found in the nucleus; however, HIV-1 NEF (12, 15, 18) and SIV NEF (13) are myristoylated (Fig. 1) and can associate with the plasma or other cellular membranes, which may be essential for their activity (7, 15). HIV-1 and SIV NEF bear amino acid sequence similarity to the nucleotide binding domain of $p21^{ras}$, $p60^{src}$, cyclic AMP-dependent protein kinase, and epidermal growth factor and insulin receptors (12, 27) (Fig. 1). With respect to HIV-1 NEF, GTP-binding and GTP-cleaving activities have been reported (12, 13); however, others have been unable to detect these activities (18). HIV-1 NEF has been reported to exhibit autophosphorylation activities (12), which indicates that NEF may be able to phosphorylate other regulatory proteins in a signal pathway into the nucleus. Recently, it was found that HIV-1 NEF can downregulate the binding of a proliferation-associated DNA binding protein in nontransformed human T lymphocytes (11). Thus, NEF may act as a signal transducer to either facilitate the binding of negative cellular factors or inhibit the binding of positive cellular factors of transcription.

We have begun to examine the replication of SIV NEF^+ and SIV NEF^- viruses in rhesus macaque primary lymphocytes; preliminary results indicate downregulatory effects exerted by NEF early after infection, which is consistent with the data presented in this manuscript. However, the role of NEF in vivo has yet to be examined. It is possible that NEF may be contributing significantly to the establishment and maintenance of viral latency exhibited by infected humans and macaques. However, downregulation of viral expression may actually contribute to disease progression in that NEF may be required for persistent infection. That is, if *nef*-negative viruses replicate unchecked, heavily infected cells may die and a swift, immune response may clear circulating virus. However, cells infected with *nef*-positive viruses may persist because virus replication is suppressed and thereby provide a virus reservoir. It should be noted that the subtle effects of NEF on transcription were determined in cell culture and that the ability of NEF to downregulate virus expression in living organisms may be more substantial. Studies of macaques infected with SIV *nef*-positive and *nef*-negative viruses will be crucial for determining the physiologic role of NEF in virus expression and disease progression (23).

ACKNOWLEDGMENTS

We thank Jeffrey Milbrandt for experimental advice on nuclear run-on assays and critical review of the manuscript, Lisa Westfield and Evan Sadler (Howard Hughes Medical Institution) for oligonucleotides, and G. Viglianti for sharing unpublished data.

This work was supported by contracts DAMD-87C-7107 and DAMD-90C-0125 from the U.S. Army Medical Research Acquisition Activity, Public Health Service grant AI24745, and training grant HL 07088-15 (to T.M.J.N.) from the National Institutes of Health. Lee Ratner is an American Cancer Society Research Professor.

REFERENCES

1. **Ahmad, N., and S. Venkatesan.** 1988. Nef protein of HIV-1 is a transcriptional repressor of HIV-1 LTR. Science **241**:1481–1485.
2. **Cheng-Mayer, C., P. Lannello, K. Shaw, P. A. Luciw, and J. A. Levy.** 1989. Differential effects of nef on HIV replication: implications for viral pathogenesis in the host. Science **246:** 1629–1632.
3. **Chirgwin, J. B., A. E. Przybyla, R. J. MacDonald, and W. J. Rutter.** 1979. Isolation of biologically active ribonucleic acid from sources enriched in ribonuclease. Biochemistry **18:**5294–5299.
4. **Cleveland, D. W., M. A. Lopata, R. J. MacDonald, N. J. Cowan, W. J. Rutter, and M. W. Kirschner.** 1980. Number and evolutionary conservation of alpha- and beta-tubulin and cytoplasmic beta- and gamma-actin genes using specific cloned cDNA probes. Cell **20:**95–105.
5. **Daniel, M. D., N. L. Letvin, N. W. King, M. Kannagi, P. K. Sehgal, R. D. Hunt, P. J. Kanki, M. Essex, and R. C. Desrosiers.** 1985. Isolation of T-cell tropic HTLV-III like retrovirus from macaques. Science **228:**1201–1204.
6. **Fisher, A. G., E. Collalti, L. Ratner, R. C. Gallo, and F. Wong-Staal.** 1985. A molecular clone of HTLV-III with biological activity. Nature (London) **316:**262–265.
7. **Franchini, G., M. Robert-Guroff, J. Ghrayeb, N. T. Chang, and F. Wong-Staal.** 1986. Cytoplasmic localization of the HTLV-III 3'orf protein in cultured T cells. Virology **155:**593–599.
8. **Gallo, R. C., F. Wong-Staal, L. Montagnier, W. A. Haseltine, and M. Yoshida.** 1988. HIV/HTLV gene nomenclature. Nature

(London) **333**:504.

9. **Gama Sosa, M. A., R. DeGasperi, L. D. Bernard, J. Hall, F. Fazely, and R. M. Ruprecht.** 1990. VI International Conference on AIDS (San Francisco), abstr. FA227.
10. **Gorman, C. M., L. F. Moffat, and B. H. Howard.** 1982. Recombinant genomes which express chloramphenicol acetyltransferase in mammalian cells. Mol. Cell. Biol. **2**:1044–1051.
11. **Guy, B., R. B. Acres. M. P. Kieny, and J.-P. Lecocq.** 1990. DNA binding factors that bind to the negative regulatory element of the human immunodeficiency virus type 1: regulation by nef. J. Acquired Immune Defic. Syndr. **3**:797–809.
12. **Guy, B., M. P. Kieny, Y. Riviere, C. LePeuch, K. Dott, M. Girard, L. Montagnier, and J. P. Lecocq.** 1987. HIV F/3′orf encodes a phosphorylated GTP-binding protein resembling an oncogene product. Nature (London) **330**:266–269.
13. **Guy, B., Y. Riviere, K. Dott, A. Regnault, and M. P. Kieny.** 1990. Mutational analysis of the HIV nef protein. Virology **176**:413–425.
14. **Hahn, B. H., L. I. Kong, S.-W. Lee, P. Kumar, M. E. Taylor, S. K. Arya, and G. M. Shaw.** 1987. Relation of HTLV-4 to simian and human immunodeficiency-associated viruses. Nature (London) **330**:184–186.
15. **Hammes, S. R., E. P. Dixon, M. H. Malim, B. R. Cullen, and W. C. Greene.** 1989. Nef protein of human immunodeficiency virus type 1: evidence against its role as a transcriptional inhibitor. Proc. Natl. Acad. Sci. USA **86**:9549–9553.
16. **Hermann, R., A. Ludwigsen, M. Chuah, R. Brack-Werner, B. Kohleisen, A. Kleinschmidt, and V. Erfle.** 1990. VI International Conference on AIDS (San Francisco), abstr. FA302.
17. **Josephs, S. F., G. Chan, L. Ratner, and F. Wong-Staal.** 1984. Human proto-oncogene nucleotide sequences corresponding to the transforming region of simian sarcoma virus. Science **223**: 487–490.
18. **Kaminchik, J., N. Bashan, D. Pinchasi, B. Amit, N. Sarver, M. I. Johnston, M. Fischer, Z. Yavin, M. Gorecki, and A. Panet.** 1990. Expression and biochemical characterization of human immunodeficiency virus type 1 *nef* gene product. J. Virol. **64**:3447–3454.
19. **Kim, S., R. Ikeuchi, R. Byrn, J. Groopman, and D. Baltimore.** 1989. Lack of a negative influence on viral growth by the nef gene of human immunodeficiency virus type 1. Proc. Natl. Acad. Sci. USA **86**:9544–9548.
20. **Luciw, P. A., C. Cheng-Mayer, and J. A. Levy.** 1987. Mutational analysis of the human immunodeficiency virus: the orf-B region down-regulates virus replication. Proc. Natl. Acad. Sci. USA **84**:1434–1438.
21. **Mulligan, R. C., and P. Berg.** 1980. Expression of a bacterial gene in mammalian cells. Science **209**:1422–1427.
22. **Myers, G., A. B. Rabson, J. A. Berzofsky, T. F. Smith, and F. Wong-Staal (ed.).** 1990. Theoretical biology and biophysics, p. II69–II70. Los Alamos Laboratory, Los Alamos, N.Mex.
23. **Naidu, Y. M., H. S. Kestler III, Y. Li, C. V. Butler, D. P. Silva, D. K. Schmidt, C. D. Troup, P. K. Sehgal, P. Sonigo, M. D. Daniel, and R. C. Desrosiers.** 1988. Characterization of infectious molecular clones of simian immunodeficiency virus (SIVMAC) and human immunodeficiency virus type 2: persistent infection of rhesus monkeys with molecularly cloned SIVMAC. J. Virol. **62**:4691–4696.
24. **Niederman, T. M. J., B. J. Thielan, and L. Ratner.** 1989. Human immunodeficiency virus type 1 negative factor is a transcriptional silencer. Proc. Natl. Acad. Sci. USA **86**:1128–1132.
25. **Ratner, L., W. Haseltine, R. Patarca, K. J. Livak, B. Starcich, S. F. Josephs, E. R. Doran, J. A. Rafalski, E. A. Whitehorn, K. Baumeister, L. Ivanoff, S. R. Petteway, Jr., M. L. Pearson, J. A. Lautenberger, T. S. Papas, J. Ghrayeb, N. T. Chang, R. C. Gallo, and F. Wong-Staal.** 1985. Complete nucleotide sequence of the AIDS virus, HTLV-III. Nature (London) **313**:277–284.
26. **Ratner, L., B. Starcich, S. F. Josephs, B. H. Hahn, E. P. Reddy, K. J. Livak, S. R. Petteway, Jr., M. L. Pearson, W. A. Haseltine, S. K. Arya, and F. W. Staal.** 1985. Polymorphism of the 3′ open reading frame of the virus associated with the acquired immune deficiency syndrome, human T-lymphotropic virus type III. Nucleic Acids Res. **13**:8219–8229.
27. **Samuel, K. P., A. Seth, A. Konopka, J. A. Lautenberger, and T. S. Papas.** 1987. The 3′orf protein of human immunodeficiency virus shows structural homology with the phosphorylation domain of human interleukin-2 receptor and the ATP-binding site of the protein kinase family. FEBS Lett. **218**:81–86.
28. **Terwilliger, E., J. G. Sodroski, C. A. Rosen, and W. A. Haseltine.** 1986. Effects of mutations within the 3′ *orf* open reading frame region of human T-cell lymphotropic virus type III (HTLV-III/LAV) on replication and cytopathogenicity. J. Virol. **60**:754–760.
29. **Viglianti, G. A., P. L. Sharma, and J. I. Mullins.** 1990. Simian immunodeficiency virus displays complex patterns of RNA splicing. J. Virol. **64**:4207–4216.